Choroidal Hyperreflective Foci Represent a Common Finding Across Different Types of Macular Atrophy

Lorena Ulla,[1,2] Claudio Foti,[1,2] Alessandro Arrigo,[3,4] Maurizio Battaglia Parodi,[3,4] Maria Vittoria Cicinelli,[3,4] Paola Marolo,[1,2] Elisabetta Miserocchi,[3,4] Mario Peronetti,[3,4] Francesco Bandello,[3,4] Enrico Borrelli,[1,2,5] and Michele Reibaldi[1,2]

[1]Department of Surgical Sciences, University of Turin, Turin, Italy
[2]Department of Ophthalmology, "City of Health and Science" Hospital, Turin, Italy
[3]Vita-Salute San Raffaele University Milan, Italy
[4]IRCCS San Raffaele Scientific Institute, Milan, Italy
[5]Department of Ophthalmology, Faculty of Medicine, Biruni University, İstanbul, Turkey

Correspondence: Enrico Borrelli, Division of Ophthalmology, Department of Surgical Sciences, University of Turin, Via Cherasco, 23, Turin 10126, Italy; borrelli.enrico@yahoo.com.

EB and MR are co-senior authors.

Received: February 12, 2025
Accepted: May 21, 2025
Published: June 13, 2025

Citation: Ulla L, Foti C, Arrigo A, et al. Choroidal hyperreflective foci represent a common finding across different types of macular atrophy. *Invest Ophthalmol Vis Sci.* 2025;66(6):42. https://doi.org/10.1167/iovs.66.6.42

Purpose. To evaluate the presence, distribution, and potential implications of choroidal hyperreflective foci (HRFs) across different types of macular atrophy and their relationship with the size of atrophic regions.

Methods. This retrospective case series analyzed 95 eyes from 87 patients with macular atrophy caused by various conditions, including geographic atrophy due to age-related macular degeneration, pachychoroid disease, punctate inner choroidopathy, angioid streaks, and Stargardt disease. Structural optical coherence tomography (OCT) images were evaluated to identify HRFs in different choroidal layers. HRF counts were correlated with the size of macular atrophy and underlying conditions using multiple regression analysis.

Results. HRFs were observed in all cases, with their number significantly associated with the size of macular atrophy ($P < 0.001$). The highest HRF counts were found in Stargardt disease, while the lowest were in pachychoroid disease. However, no association was identified between HRF quantity and specific disease type ($P = 0.2$). HRFs were primarily located in the choriocapillaris, Sattler's layer, and near Bruch's membrane but were absent within choroidal vessels.

Conclusions. HRFs represent a common OCT finding in various disorders associated with macular atrophy. Their quantity correlates with atrophy size rather than disease type, suggesting they are likely normal choroidal components rendered visible by RPE loss. Future studies are warranted to elucidate their origin and potential implications for disease progression.

Keywords: choroid, macular atrophy, age-related macular degeneration, hyperreflective foci, retinal dystrophy

Choroidal hyperreflective foci (HRFs) were first identified by Piri et al.[1] in patients with macular atrophy secondary to Stargardt disease. These features appeared on structural optical coherence tomography (OCT) as circular or oval high-reflectivity structures, typically ranging from 10 to 50 µm in diameter, as observed on spectral-domain OCT images without contrast adjustment in the latter study. Their location was generally adjacent to vascular borders, while they were not observed within the vessels' lumen. The latter study concluded that these choroidal HRFs may be specific to patients with Stargardt disease.

Subsequently, our group reported choroidal HRFs in patients with geographic atrophy (GA) secondary to age-related macular degeneration (AMD).[2] These choroidal HRFs in GA shared a similar distribution pattern to those observed in Stargardt disease, being located adjacent to Bruch's membrane or along blood vessel borders, with none detected within choroidal vessels. Most of these hyperreflective deposits were concentrated in regions corresponding to areas with complete RPE and outer retinal atrophy (cRORA), with a significant correlation between the extent of atrophy and the number of choroidal HRFs. Interestingly, the size and shape of these deposits varied, with smaller, round structures near Bruch's membrane and larger, oval deposits in deeper choroidal layers.

The presence of choroidal HRFs in both GA and Stargardt disease suggests that these features might serve as general markers of macular atrophy rather than being specific to a single disease. Their visibility may be enhanced in areas of RPE atrophy due to increased signal penetration resulting from the absence of the RPE layer. The aim of this study was thus to describe the presence and distribution of choroidal HRFs across various conditions associated with macular atrophy, including AMD, pachychoroid disease, punctate inner

choroidopathy (PIC), angioid streaks, and retinal dystrophies. Specifically, we examined the relationship between choroidal HRF presence and amount across different types of macular atrophy and correlated these findings with the size of the atrophic area.

Methods

This study adhered to the 1964 Declaration of Helsinki and its later amendments. All patients involved signed an informed consent form approved by the local ethics committee.

Participants

This retrospective case series included patients with macular atrophy caused by various conditions, such as AMD, pachychoroid disease, PIC, angioid streaks, and retinal dystrophies.[3–10] The patients were retrospectively recruited from the Department of Ophthalmology at Città della Salute e della Scienza Hospital in Turin and the San Raffaele Hospital in Milan, Italy. Diagnoses were established using well-defined criteria previously detailed in the literature.[9,11–19]

Patients with angioid streaks were included regardless of the underlying disease causing these features. To be included, patients needed to have a region of RPE atrophy measuring at least 250 µm, displaying OCT features consistent with cRORA.[20]

At the inclusion visit, the following exclusion criteria were applied to the study eye: (1) presence of fibrotic macular neovascularization obstructing choroidal visualization; (2) a history of retinal surgery, including cataract surgery; and (3) a history or evidence of other retinal or optic nerve disorders. Additionally, eyes where choroidal layer differentiation was not feasible on OCT during analysis were excluded.

Structural OCT was performed with the Heidelberg Spectralis HRA+OCT device (Heidelberg Engineering, Heidelberg, Germany). The spectral-domain OCT imaging session included 19 horizontal B-scans covering approximately a 5.5 × 4.5-mm area (20° × 15°) centered on the fovea. Each B-scan was composed of 25 automated real-time averaging OCT images. A quality via signal-to-noise ratio of 25 was required for the OCT images to be included, as recommended by the manufacturer.[21]

OCT Grading

Structural OCT images were initially assessed for eligibility by an experienced and certified grader (EB). The study included only volumetric scans where the choroid was fully visible across all B-scans.

To identify the different choroidal layers and count choroidal hyperreflective foci, a previously validated methodology was employed.[2] Specifically, Haller's layer was defined as the outermost portion of the choroid containing larger choroidal vessels. Sattler's layer was described as the region housing medium-sized choroidal vessels, appearing as intermediate-sized, less prominent spaces within a denser stromal background. The choriocapillaris (CC) was identified as the least reflective layer, situated above Sattler's layer and adjacent to Bruch's membrane.[2] After delineating the choroidal layers, each B-scan for each eye was independently assessed by a certified grader (EB) for the presence and quantity of HRFs within these layers. HRFs were defined as circular or oval structures with high reflectivity, appearing black on inverted images and white on noninverted images, with diameters ranging from 10 to 50 µm. Identification and counting were performed using high-magnification white-on-black SD-OCT images, a technique previously recommended to enhance the visualization of HRFs in the choroid.[1] In addition to the quantitative grading, the grader also evaluates the images qualitatively to determine whether these foci show a topographical preference in relation to the presence of RPE atrophy. Specifically, the focus is on whether the number of foci is higher in areas with cRORA compared to those without cRORA.

The graders utilized the built-in software to measure the area of RPE atrophy on near-infrared reflectance images, as previously described.[22,23]

Statistical Analysis

Statistical calculations were performed using Statistical Package for Social Sciences (version 23.0.0.0; SPSS, Chicago, IL, USA).

The analysis included descriptive statistics for demographics and main clinical data, as well as qualitative descriptions of the imaging characteristics. Moreover, the data were grouped according to the choroidal layer analyzed, and quantitative values were reported as mean ± SD. Quantitative data were examined to assess their normal distribution. Independent-samples Mann–Whitney *U* test was employed to compare different groups.

A multiple regression analysis with number of choroidal HRFs as the dependent variable was applied, adjusting for age, gender, and disease-causing macular atrophy.

Results

We analyzed a total of 87 patients (95 eyes) with macular atrophy resulting from various disorders. In detail, 41 participants (49 eyes) were affected by GA and AMD, 9 had angioid streaks, 10 had pachychoroid disease, 12 had either active or inactive PIC, 4 had retinitis pigmentosa (RP), and 11 had Stargardt disease (Figs. 1–7). The mean age of the participants was 72.0 ± 17.8 years (Table 1). The size of macular atrophy differed significantly across disease categories. It was the greatest in Stargardt disease and the smallest in pachychoroid disease ($P < 0.0001$).

Considering the entire OCT volume and full thickness of the choroid (i.e., without regard to specific choroidal layers), the mean ± SD number of choroidal HRFs was 366 ± 146 in GA, 223 ± 105 in angioid streaks, 120 ± 31 in pachychoroid disease, 182 ± 130 in PIC, 172 ± 123 in RP, and 494 ± 408 in Stargardt disease ($P < 0.0001$; Table 2). These results indicated that the amount of choroidal HRFs was the highest in Stargardt disease and the lowest in pachychoroid disease. Table 2 presents the results based on the number of choroidal HRFs observed per single B-scan. Table 3 shows the distribution of choroidal HRFs across the various layers of the choroid (i.e., CC, Sattler's and Haller's layers; Supplementary Fig. S1).

Regression Analysis With Amount of Choroidal HRFs as the Dependent Variable

Qualitatively, choroidal HRFs were more abundant in the cRORA regions compared to the non-cRORA regions (Fig. 7). Accordingly, the multiple regression analysis revealed that the total number of HRFs in the entire choroid (depen-

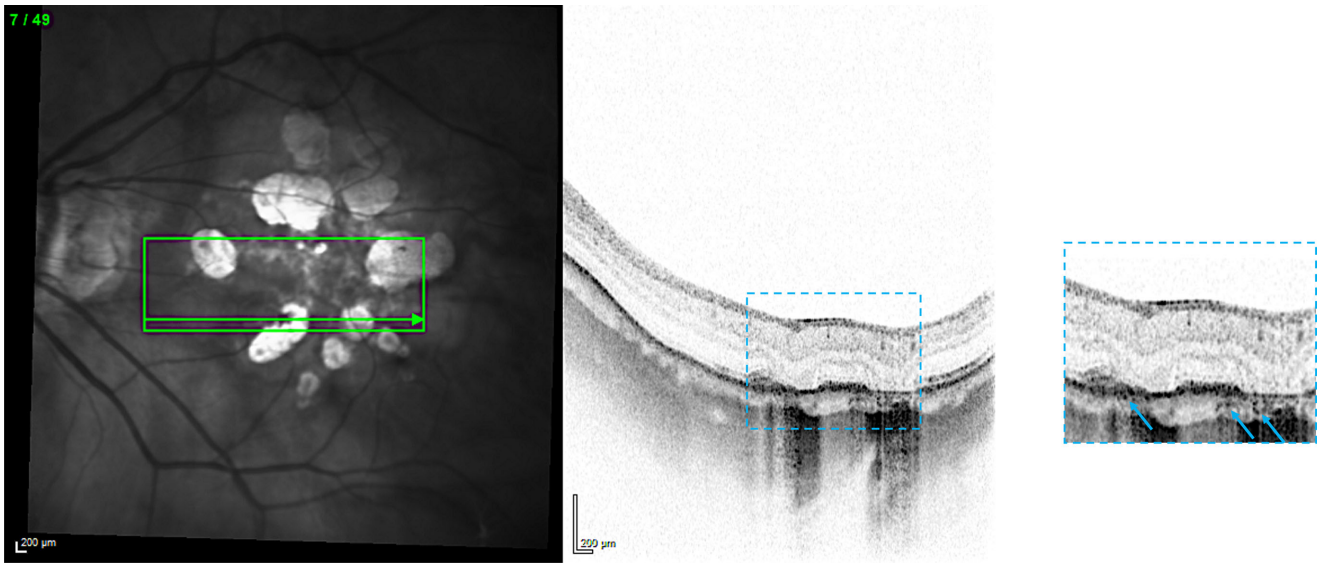

Figure 1. Representative OCT B-scan from a patient with PIC. The OCT B-scan (*left*) shows the presence of choroidal HRFs. A magnified visualization of the region with RPE atrophy is reported in the *right column*. *Cyan arrows* highlight some of the choroidal HRFs.

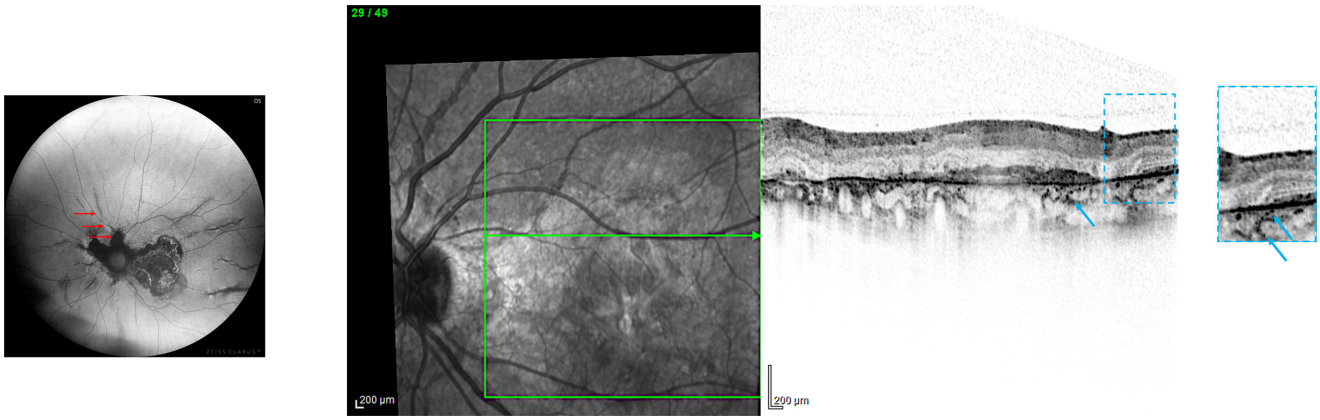

Figure 2. Representative OCT B-scan from a patient with angioid streaks. The green fundus autofluorescence image (*left*) highlights peripapillary hypoautofluorescent areas associated with angioid streaks (one is highlighted with *red arrows*). The OCT B-scan (*middle*) reveals the presence of choroidal HRFs. A magnified view of the region of interest is provided in the *right column* for enhanced visualization. *Cyan arrows* highlight some of the choroidal HRFs.

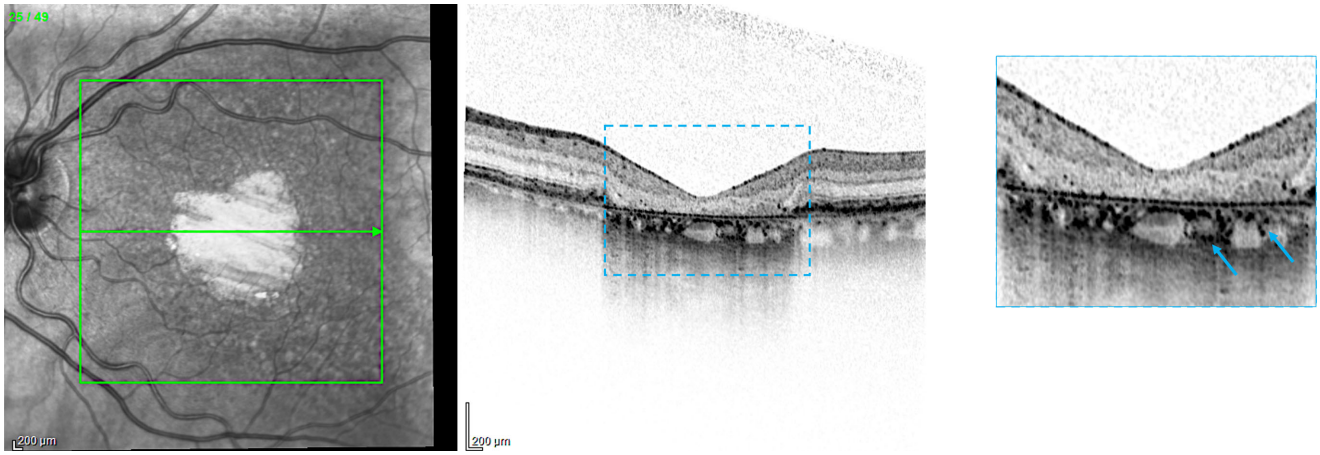

Figure 3. Representative OCT B-scan from a patient with GA. The OCT B-scan (*left*) demonstrates choroidal HRFs in the foveal region affected by GA secondary to AMD. A magnified view of the foveal region is shown in the *right column* for detailed visualization. *Cyan arrows* highlight some of the choroidal HRFs.

Investigative Ophthalmology & Visual Science

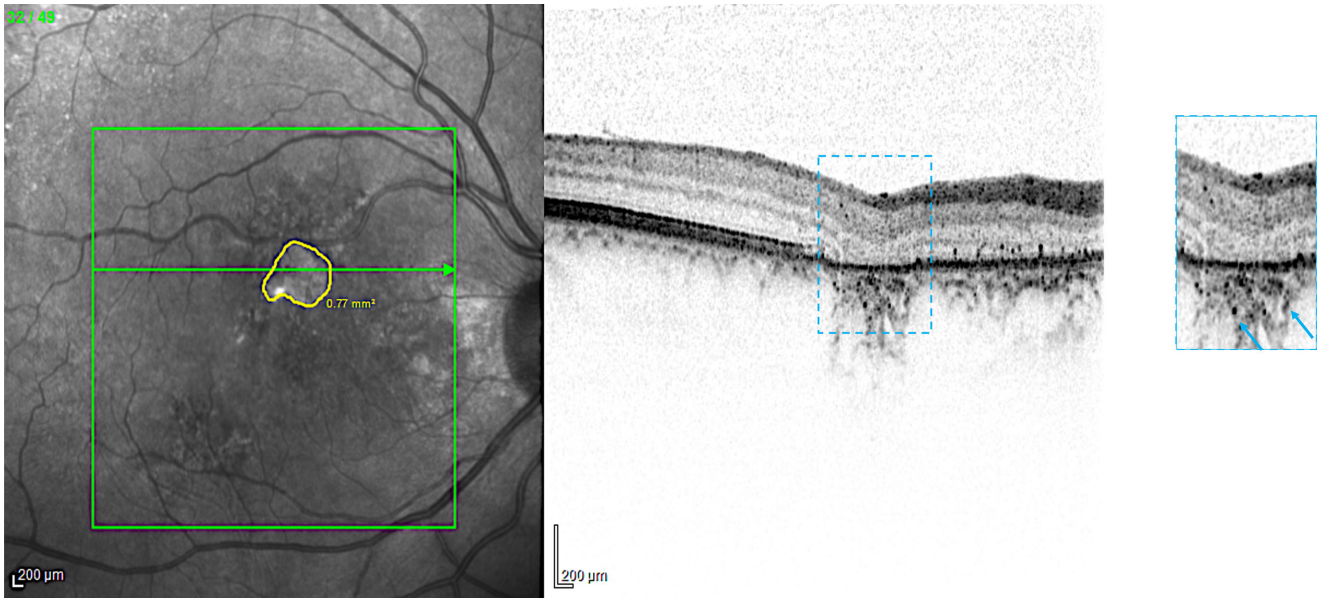

Figure 4. Representative OCT B-scan from a patient with pachychoroid disease. The OCT B-scan image (*left*) shows a region of RPE atrophy associated with pachyvessels in the choroid, along with choroidal HRFs in the surrounding stromal tissue. A magnified view of the region with RPE atrophy is provided in the *right column* for detailed assessment. *Cyan arrows* highlight some of the choroidal HRFs.

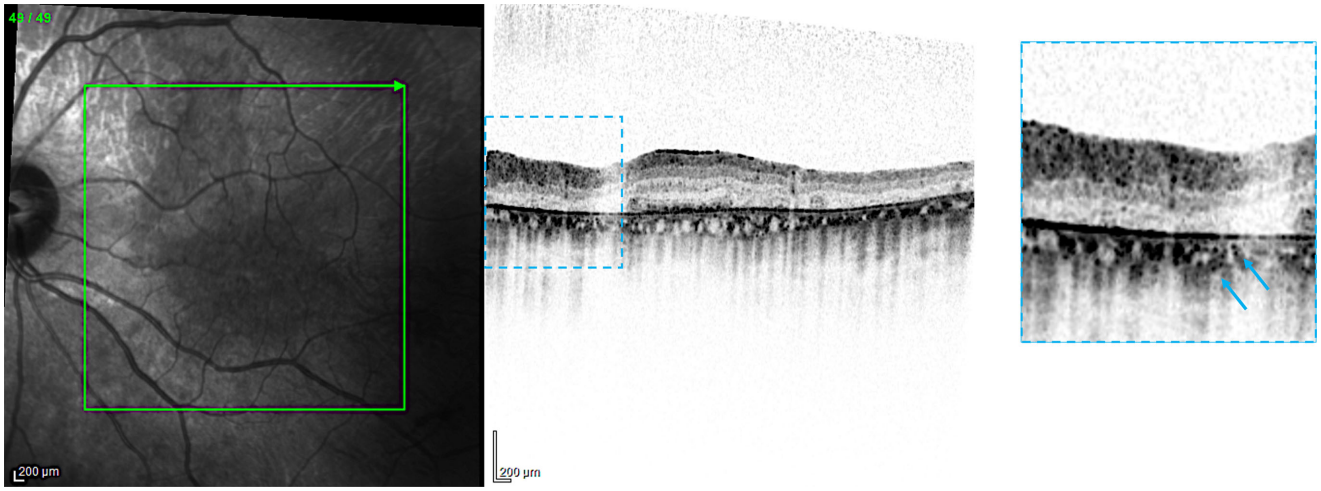

Figure 5. Representative OCT B-scan from a patient with retinitis pigmentosa. The OCT B-scan image (*left*) displays a region of RPE atrophy accompanied by a thin choroid, with choroidal HRFs observed in the surrounding stromal tissue. A magnified view of the region with RPE atrophy is presented in the *right column* for closer examination. *Cyan arrows* highlight some of the choroidal HRFs.

dent variable) was significantly associated with the size of macular atrophy ($P < 0.001$; standardized estimate = 2.383). No significant associations were identified with the disease-causing macular atrophy ($P = 0.185$; SE = 10.424) or gender ($P = 0.572$; SE = 21.052). A marginal association was found with age, with increased age associated with a reduced number of choroidal HRFs ($P = 0.079$; SE = 1.018) (Table 4).

Discussion

In this study, we examined the prevalence and characteristics of choroidal HRFs in patients with macular atrophy secondary to various chorioretinal disorders associated with macular atrophy, including AMD, pachychoroid disease, PIC, angioid streaks, and retinal dystrophies. Overall, we demonstrated that these choroidal features are prevalent across various disorders, suggesting that they may represent normal features of the choroid, which become more visible due to the absence of RPE caused by atrophy.

Choroidal HRFs have been described in healthy patients, with a higher density in the central macular region than in the periphery.[24] More importantly, prior studies have documented choroidal HRFs using structural OCT in different pathological conditions characterized by macular atrophy (i.e., Stargardt disease[1] and GA[2]). In detail, Piri et al.[1] performed a retrospective review of 26 eyes from 13 patients with Stargardt disease, revealing choroidal HRFs in all cases and finding a positive correlation between HRFs in the CC and Sattler's layer with disease progression. Based on their findings, the authors proposed that choroidal HRFs in Star-

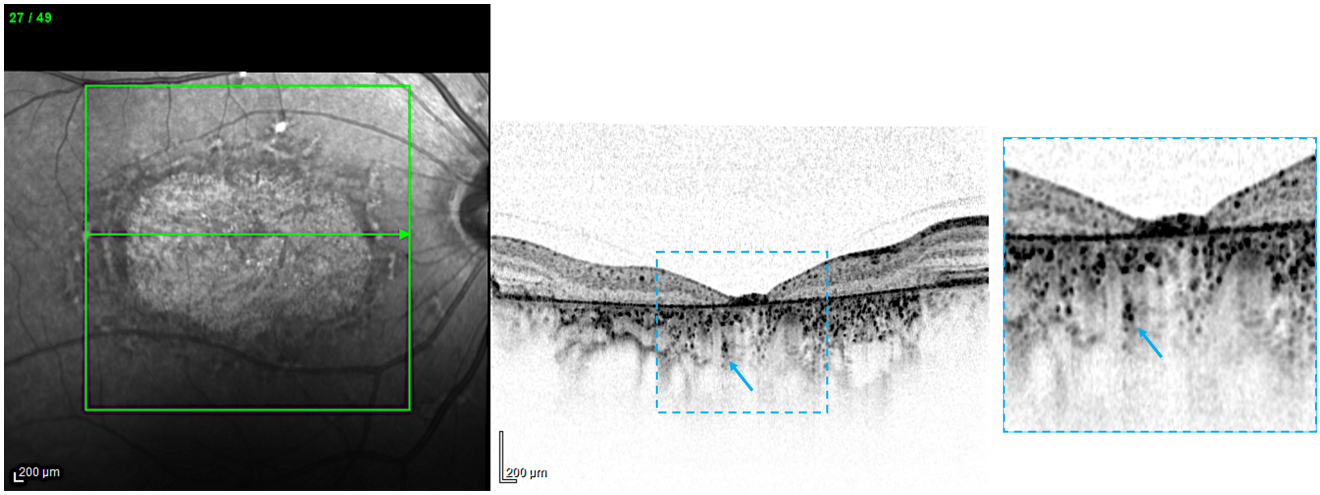

Figure 6. Representative OCT B-scan from a patient with Stargardt disease. The OCT B-scan image (*left*) shows an extensive region of RPE atrophy involving the fovea, with choroidal HRFs visible in the choroid. A magnified view of the foveal region is provided in the *right column* for detailed assessment. *Cyan arrows* highlight some of the choroidal HRFs.

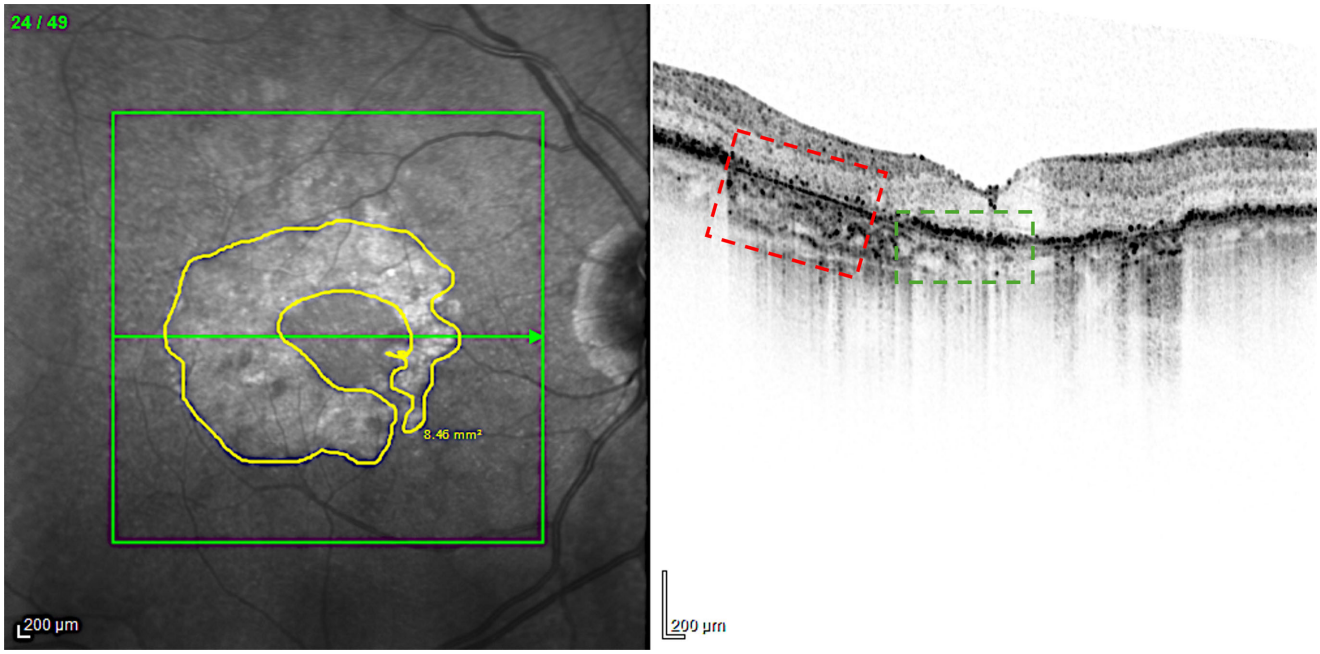

Figure 7. Representative OCT B-scan from a patient with GA. The OCT B-scan image reveals choroidal foci in both atrophic regions (highlighted by a *red dashed box*) and nonatrophic regions (highlighted by a *green dashed box*), although their presence is less prominent in the latter.

gardt disease might represent the movement of lipofuscin deposits from the outer retina to the choroid as part of the degenerative process.

Finally, choroidal HRFs have recently been identified as a biomarker for leukemic choroidopathy.[25]

Successively, our group has noted the presence of choroidal HRFs in GA.[2] In the latter study, we have provided both qualitative and quantitative analyses of choroidal HRFs. In detail, in a cohort of 49 eyes diagnosed with GA, choroidal HRFs were observed in all cases, primarily in the CC and Sattler's layers. Additionally, the latter study indicated a direct relationship between the amount of choroidal HRFs and the size of GA, suggesting that larger GA areas are associated with a higher amount of choroidal HRFs. We speculated that some choroidal HRFs observed at the level of Bruch's membrane in GA may serve as imaging surrogates for "dissociated" RPE cells previously identified in histologic studies of patients with AMD.[26,27] However, since choroidal HRFs are not unique to GA in AMD, and given our findings of a direct correlation between the quantity of choroidal HRFs and the size of GA, we may suggest that choroidal HRFs may be a general choroidal response simply related to development and progression of GA, independently of the specific disease. Alternatively, they could be normal components of the choroid that become visible in GA eyes due to enhanced signal penetration caused by the absence of the RPE layer.[2]

Investigative Ophthalmology & Visual Science

Table 1. Age of Patients Included in the Analysis

Characteristic	AMD ($n = 49$)	Angioid Streaks ($n = 9$)	Pachychoroid Disease ($n = 10$)	PIC ($n = 12$)	RP ($n = 4$)	Stargardt Disease ($n = 11$)
Age, mean ± SD, y	82.0 ± 6.1	72.0 ± 11.0	77.3 ± 4.8	54.5 ± 11.6	68.0 ± 8.7	39.8 ± 14.5

Table 2. Number of Choroidal Foci and RPE Atrophy Area Size Across Various Disorders

Characteristic	Number of Choroidal Foci		RPE Atrophy Area, mm^2
	B-Scan	Entire OCT Volume	
AMD ($n = 49$)	19.1 ± 7.9	366 ± 146	5.97 ± 7.97
Angioid streaks ($n = 9$)	12.6 ± 5.5	223 ± 105	3.03 ± 5.55
Pachychoroid disease ($n = 10$)	11.9 ± 1.6	120 ± 31	1.72 ± 1.65
PIC ($n = 12$)	10.5 ± 5.4	182 ± 130	2.87 ± 2.17
RP ($n = 4$)	9.1 ± 6.5	172 ± 123	2.99 ± 1.78
Stargardt disease ($n = 11$)	26.0 ± 21.5	494 ± 408	7.47 ± 7.38

Table 3. Number of Choroidal Foci Within the Different Choroidal Layers Across Various Disorders

Characteristic	Number of Choroidal Foci		
	Chorocapillaris	Sattler's Layer	Haller's Layer
AMD ($n = 49$)	194 ± 85	134 ± 61	29 ± 17
Angioid streaks ($n = 9$)	115 ± 60	100 ± 60	28 ± 17
Pachychoroid disease ($n = 10$)	77 ± 24	40 ± 20	12 ± 8
PIC ($n = 12$)	103 ± 41	52 ± 35	17 ± 17
RP ($n = 4$)	98.7 ± 74.5	58.7 ± 37.7	15.5 ± 12
Stargardt disease ($n = 11$)	245.9 ± 182	204 ± 190.6	41 ± 45.6

Table 4. Results of Multivariable Analysis With Number of Choroidal HRFs as the Dependent Variable

Characteristic	Estimate (95% CI)	Standard Estimate	*P* Value
Age	−1.8121 (−3.835 to 0.211)	1.018	0.079
Gender	11.9518 (−29.878 to 53.782)	21.052	0.572
Choroidal thickness	0.0768 (−0.214 to 0.367)	0.146	0.601
Size of RPE atrophy	44.1058 (39.370 to 48.841)	2.383	<0.001
Disease	−13.9325 (−34.645 to 6.780)	10.424	0.185

CI, confidence interval.

However, these OCT features were not described only in disorders typically characterized by macular atrophy. In detail, Roy et al.[28] conducted a retrospective analysis of 119 eyes from 60 patients with diabetic macular edema, finding choroidal HRFs in 59 eyes (49.5% of the sample). They proposed that these HRFs may arise from the migration of neuroretinal HRFs into the choroid, supported by the observation that all 59 eyes with choroidal HRFs also exhibited neuroretinal HRFs. These findings suggest that the origin of choroidal HRFs may be more complex and remains to be fully understood.

In this study, we contribute to the literature by evaluating choroidal HRFs across various forms of macular atrophy. Within our cohort, choroidal HRFs were observed in all patients. Notably, as previously demonstrated in studies on Stargardt disease[1] and GA,[2] these choroidal HRFs are primarily located at the level of Bruch's membrane, the CC, and Sattler's layer, with HRFs seen in the choroidal stroma but absent within the choroidal vessels.

This study included cases with various disorders (i.e., AMD, pachychoroid disease, PIC, angioid streaks, and retinal dystrophies) to investigate whether the underlying disease associated with macular atrophy could affect the presence and quantity of choroidal HRFs. This approach aimed to clarify the origins of these findings, as variations between disorders might indicate a disorder-specific origin. In our cohort, the amount of choroidal HRFs was highest in Stargardt disease and lowest in pachychoroid disease. Based on these observations, we hypothesized that the underlying disease driving the macular atrophy might influence the amount of choroidal HRFs. In pachychoroid disease, the increased vascular permeability associated with the condition may create a masking effect on choroidal foci, potentially explaining the lower number of foci observed in this pathology.

We then performed a multivariate regression analysis, using choroidal HRF quantity as the dependent variable and both disease type and macular atrophy size as independent variables. Interestingly, this analysis revealed that the only variable associated with choroidal HRF quantity was the size of RPE atrophy, while the specific disease type showed no association. This finding appears to further suggest that choroidal HRFs may be a natural component of the choroid, with their visualization enhanced due to the absence of

Investigative Ophthalmology & Visual Science

the RPE. Alternatively, or in conjunction, choroidal HRFs may reflect a generalized response to macular atrophy, regardless of the underlying disease. If the latter theory is correct, although in the absence of clear histopathologic characterizations, we may speculate that choroidal HRFs could represent macrophage aggregates involved in the inflammatory process associated with choroidal changes during atrophy progression and expansion. In a previous study, Parodi et al.[29] found that choroidal HRFs are significantly increased during the active, pre-reactive, and reactive phases in patients with angioid streaks, serving as valuable markers for monitoring choroidal neovascularization (CNV) activity. Based on this, we may speculate that macrophage aggregates play a role in the complex pathogenetic mechanisms underlying both CNV development and progression, as well as RPE atrophy formation and expansion.[29,30]

As previously noted, the correlation between the size of RPE atrophy and the number of choroidal HRFs may indicate that these HRFs represent melanocytes.[31–36] It is well established that choroidal blood vessels are enveloped by highly pigmented melanocytes, which may become exposed and more visible when the RPE is absent due to macular atrophy. Importantly, the number of melanocytes in both the body and the choroid declines with age,[37] which may help explain the borderline statistical significance observed between the number of choroidal HRFs and age (i.e., inverse relationship) in our multivariable analysis. Finally, choroidal HRFs may represent remnants of endothelial cells from the choriocapillaris or RPE following damage in the context of macular atrophy.[38,39]

Our study had a number of limitations. First, we did not perform correlation analyses between imaging and histologic findings—an important area for future research to address to clarify the underlying mechanisms and implications of this phenomenon. Second, choroidal foci and atrophic areas were identified and quantified manually, introducing potential errors in the counting process. However, previous studies have shown this manual process to be consistent and repeatable, even when compared to an automated method.[2] More importantly, this was a retrospective study, and the volumetric scans available for our patients did not permit en face visualization. En face imaging has been demonstrated to be a reliable and effective method for detecting choroidal HRFs in normal eyes.[24] Therefore, future studies incorporating en face imaging are warranted to further explore this finding. Finally, all imaging techniques contain artifacts that could significantly affect the processing and interpretation of quantitative data, potentially compromising their reliability.[40]

In conclusion, this OCT study shows that HRFs can be visualized in the choroid of patients with various retinal pathologies that cause macular atrophy, with HRFs observed across all choroidal layers. The primary factor influencing the amount of choroidal HRFs is the size of macular atrophy, suggesting that these OCT findings likely represent normal choroidal components that become more visible due to the absence of the RPE. Future studies that correlate histology with imaging are essential for a deeper understanding of the mechanisms behind the formation and visualization of choroidal HRFs. Additionally, research utilizing longitudinal data could determine whether choroidal HRFs change over time and clarify their relationship to disease progression and growth patterns.

Acknowledgments

Disclosure: **L. Ulla**, None; **C. Foti**, None; **A. Arrigo**, None; **M. Battaglia Parodi**, None; **M.V. Cicinelli**, None; **P. Marolo**, None; **E. Miserocchi**, None; **M. Peronetti**, None; **F. Bandello**, None; **E. Borrelli**, None; **M. Reibaldi**, None

References

1. Piri N, Nesmith BLW, Schaal S. Choroidal hyperreflective foci in Stargardt disease shown by spectral-domain optical coherence tomography imaging: correlation with disease severity. *JAMA Ophthalmol*. 2015;133(4):398–405.
2. Borrelli E, Reibaldi M, Barresi C, Berni A, Introini U, Bandello F. Choroidal hyper-reflective foci in geographic atrophy. *Invest Ophthalmol Vis Sci*. 2023;64(14):5.
3. Borrelli E, Cappellani F, Pulido JS, *et al.* The umbra and the penumbra: longitudinal effects of geographic atrophy in AMD on the outer choroid by imaging analysis and histopathological correlation. *Invest Ophthalmol Vis Sci*. 2024;65(14):2.
4. Borrelli E, Barresi C, Berni A, et al. OCT risk factors for 2-year foveal involvement in non-treated eyes with extrafoveal geographic atrophy and AMD. *Graefes Arch Clin Exp Ophthalmol*. 2024;262(7):2101–2109.
5. Ramtohul P, Freund KB, Parodi MB, et al. Punctate inner pachychoroidopathy: demographic and clinical features of inner choroidal inflammation in eyes with pachychoroid disease. *Retina*. 2023;43(11):1960–1970.
6. Cicinelli MV, Montesano G, Berni A, et al. Photoreceptor integrity in MEWDS: longitudinal structure-function correlations. *Invest Ophthalmol Vis Sci*. 2024;65(4):28.
7. Cicinelli MV, Menean M, Apuzzo A, et al. Presumed Müller cell activation in multiple evanescent white dot syndrome. *Invest Ophthalmol Vis Sci*. 2023;64(13):20.
8. Bianco L, Arrigo A, Antropoli A, et al. Association between genotype and phenotype severity in ABCA4-associated retinopathy. *JAMA Ophthalmol*. 2023;141(9):826–833.
9. Arrigo A, Grazioli A, Romano F, et al. Multimodal evaluation of central and peripheral alterations in Stargardt disease: a pilot study. *Br J Ophthalmol*. 2020;104(9):1234–1238.
10. Antropoli A, Arrigo A, Bianco L, Cavallari E, Bandello F, Battaglia Parodi M. Hyperautofluorescent ring pattern in retinitis pigmentosa: clinical implications and modifications over time. *Invest Ophthalmol Vis Sci*. 2023;64(12):8.
11. Vallino V, Berni A, Coletto A, et al. Structural OCT and OCT angiography biomarkers associated with the development and progression of geographic atrophy in AMD. *Graefes Arch Clin Exp Ophthalmol*. 2024;262(11):3421–3436.
12. Borrelli E, Battista M, Gelormini F, et al. Rate of misdiagnosis and clinical usefulness of the correct diagnosis in exudative neovascular maculopathy secondary to AMD versus pachychoroid disease. *Sci Rep*. 2020;10(1):20344.
13. Du R, Fang Y, Jonas JB, et al. Clinical features of patchy chorioretinal atrophy in pathologic myopia. *Retina*. 2020;40(5):951–959.
14. Zhang X, Zuo C, Li M, Chen H, Huang S, Wen F. Spectral-domain optical coherence tomographic findings at each stage of punctate inner choroidopathy. *Ophthalmology*. 2013;120(12):2678–2683.
15. Park JG, Halim MS, Uludag G, et al. Distinct patterns of choroidal lesions in punctate inner choroidopathy and multifocal choroiditis determined by heatmap analysis. *Ocul Immunol Inflamm*. 2022;30(2):276–281.
16. Cicinelli MV, Torrioli E, La Franca L, et al. Incidence and risk factors of visual impairment in patients with angioid streaks and macular neovascularization. *Ophthalmol Retina*. 2023;7(5):431–440.

17. Tsokolas G, Tossounis C, Tyradellis S, Motta L, Panos GD, Empeslidis T. Angioid streaks remain a challenge in diagnosis, management, and treatment. *Vision (Basel)*. 2024;8(1):10.
18. Berni A, Arrigo A, Bianco L, et al. New insights in the multimodal imaging of retinitis pigmentosa. *Eur J Ophthalmol*. 2024;34(2):357–366.
19. Tee JJL, Carroll J, Webster AR, Michaelides M. Quantitative analysis of retinal structure using spectral-domain optical coherence tomography in RPGR-associated retinopathy. *Am J Ophthalmol*. 2017;178:18–26.
20. Sadda SR, Guymer R, Holz FG, et al. Consensus definition for atrophy associated with age-related macular degeneration on OCT: Classification of Atrophy Report 3. *Ophthalmology*. 2019;126(1):177.
21. Huang Y, Gangaputra S, Lee KE, et al. Signal quality assessment of retinal optical coherence tomography images. *Invest Ophthalmol Vis Sci*. 2012;53(4):2133–2141.
22. Abdelfattah NS, Sadda J, Wang Z, Hu Z, Sadda S. Near-infrared reflectance imaging for quantification of atrophy associated with age-related macular degeneration. *Am J Ophthalmol*. 2020;212:169–174.
23. Dolz-Marco R, Gal-Or O, Freund KB. Choroidal thickness influences near-infrared reflectance intensity in eyes with geographic atrophy due to age-related macular degeneration. *Invest Ophthalmol Vis Sci*. 2016;57(14):6440–6446.
24. Song MS, Kim YH, Oh J. Spatial distribution of hyperreflective choroidal foci in the macula of normal eyes. *Transl Vis Sci Technol*. 2024;13(8):35.
25. Menean M, Apuzzo A, Mastaglio S, et al. Imaging biomarkers of leukaemic choroidopathy. *Acta Ophthalmol (Copenh)*. 2023;101(5):553–559.
26. Cao D, Leong B, Messinger JD, et al. Hyperreflective foci, optical coherence tomography progression indicators in age-related macular degeneration, include transdifferentiated retinal pigment epithelium. *Invest Ophthalmol Vis Sci*. 2021;62(10):34.
27. Curcio CA, Zanzottera EC, Ach T, Balaratnasingam C, Freund KB. Activated retinal pigment epithelium, an optical coherence tomography biomarker for progression in age-related macular degeneration. *Invest Ophthalmol Vis Sci*. 2017;58(6):BIO211–BIO226.
28. Roy R, Saurabh K, Shah D, Chowdhury M, Goel S. Choroidal hyperreflective foci: a novel spectral domain optical coherence tomography biomarker in eyes with diabetic macular edema. *Asia Pac J Ophthalmol*. 2019;8(4):314–318.
29. Parodi MB, Arrigo A, Romano F, et al. Hyperreflective foci number correlates with choroidal neovascularization activity in angioid streaks. *Invest Ophthalmol Vis Sci*. 2018;59(8):3314–3319.
30. Camelo S, Raoul W, Lavalette S, et al. Delta-like 4 inhibits choroidal neovascularization despite opposing effects on vascular endothelium and macrophages. *Angiogenesis*. 2012;15(4):609–622.
31. Schmidt SY, Peisch RD. Melanin concentration in normal human retinal pigment epithelium. Regional variation and age-related reduction. *Invest Ophthalmol Vis Sci*. 1986;27(7):1063–1067.
32. Weiter JJ, Delori FC, Wing GL, Fitch KA. Retinal pigment epithelial lipofuscin and melanin and choroidal melanin in human eyes. *Invest Ophthalmol Vis Sci*. 1986;27(2):145–152.
33. McLeod DS, Taomoto M, Otsuji T, Green WR, Sunness JS, Lutty GA. Quantifying changes in RPE and choroidal vasculature in eyes with age-related macular degeneration. *Invest Ophthalmol Vis Sci*. 2002;43(6):1986–1993.
34. Dolz-Marco R, Glover JP, Gal-Or O, et al. Choroidal and subretinal pigment epithelium caverns: multimodal imaging and correspondence with Friedman lipid globules. *Ophthalmology*. 2018;125(8):1287–1301.
35. Zanzottera EC, Messinger JD, Ach T, Smith RT, Curcio CA. Subducted and melanotic cells in advanced age-related macular degeneration are derived from retinal pigment epithelium. *Invest Ophthalmol Vis Sci*. 2015;56(5):3269–3278.
36. Zanzottera EC, Messinger JD, Ach T, Smith RT, Freund KB, Curcio CA. The Project MACULA retinal pigment epithelium grading system for histology and optical coherence tomography in age-related macular degeneration. *Invest Ophthalmol Vis Sci*. 2015;56(5):3253–3268.
37. Nag TC. Ultrastructural changes in the melanocytes of aging human choroid. *Micron*. 2015;79:16–23.
38. Piskova T, Kozyrina AN, Di Russo J. Mechanobiological implications of age-related remodelling in the outer retina. *Biomater Adv*. 2023;147:213343.
39. Chirco KR, Sohn EH, Stone EM, Tucker BA, Mullins RF. Structural and molecular changes in the aging choroid: implications for age-related macular degeneration. *Eye*. 2017;31(1):10–25.
40. Arrigo A, Aragona E, Battaglia Parodi M, Bandello F. Quantitative approaches in multimodal fundus imaging: state of the art and future perspectives. *Prog Retin Eye Res*. 2023;92:101111.

Investigative Ophthalmology & Visual Science